FINE STRUCTURE AND DYNAMICS OF ROTATING MAGNETIC ISLANDS IN THE TEXTOR TOKAMAK

M.Yu.Kantor[1,2,3], A. Krämer-Flecken[1], S. Soldatov[1,4] and the TEXTOR team

[1]*Institute for Energy Research – Plasma Physics*, Forschungszentrum Jülich GmbH, Association EURATOM-FZJ, D-52425 Jülich, Germany*
[2]*FOM-Institute for Plasma Physics Rijnhuizen*, Association EURATOM-FOM, P.O. Box 1207, 3430 BE Nieuwegein, The Netherlands*
[3]*Ioffe Institute, RAS, Saint Petersburg 194021, Russia*
[4]*Department of Applied Physics, Ghent University, 9000 Gent, Belgium*
**Partners in the Trilateral Euregio Cluster*

Abstract

Local measurements of electron temperature and density across a chain of coupled magnetic islands rotating in plasma of the TEXTOR tokamak are presented in the report. The spatial structure of electron density around the x-points of the islands has been found to be essentially different from the structures of electron temperature and pressure as well as the common structure of helical magnetic perturbations in rotating islands. Such a large difference violates the coupling of the density with the magnetic flux around the x-points of rotating islands in TEXTOR.

Experimental conditions

The rotating islands were excited by AC helical currents in DED coils [1] wrapped around the central column of the TEXTOR tokamak (R=175 cm, a =45 cm). These currents create a perturbed magnetic field rotating in the toroidal direction at ~1 kHz frequency and driving magnetic islands in plasma.

Local measurements of electron temperature (T_e) and density (n_e) at a high accuracy, spatial resolution and sampling rate have become possible on TEXTOR after upgrading Thomson scattering (TS) diagnostic with a laser multipass probing system [2,3]. Profiles of T_e and n_e are measured by the TS diagnostic at the sampling rate of 5 kHz along the vertical chord (z-direction) covering the full plasma diameter of 90 cm high and shifted by ~ 4 cm outwards the magnetic axis. The scattered light collected from this chord is separated by ~ 120 independent spatial channels [4]. The statistical errors of the measurements are 2% for T_e and 1% for n_e in the plasma core.

Electron temperature was additionally measured by the ECE diagnostic [5] located in another toroidal cross section of TEXTOR. The ECE diagnostic system is equipped with a set of more then 20 frequency channels covering the full plasma diameter along the major radius. Eight ECE channels with low electrical noises (<2%) have been selected from the set and used in the analysis.

Experimental results

The dynamics of T_e and n_e measured by the TS diagnostic are shown in fig. 1a and 1b. The T_e and n_e profiles averaged over a 9 ms time interval are shown in the left hand sides of the figure sections along with the T_e and n_e variations in individual pulses located around the zero lines of these plots. The time-space domains of the variations are shown in the contour plots which reveal island structures with a resolution ~10 eV and $2*10^{17}$ m^{-3}.

Standard deviations of the T_e variations with subtracted statistical noises are plotted in fig.2 together with the similar variations measured by the ECE diagnostic along the major radius. The TS data are mapped on the horizontal axis from the upper and lower parts of the probing chord along the circular magnetic surfaces in the TEXTOR plasma. T_e fluctuations in the mid plane appear somewhat less than those in the vertical chord.

The T_e variations are pretty symmetrical in respect to the magnetic axis located at R~1.8 m and have local minima near integer q values. The q profile and the positions of the rational magnetic surfaces (q=1,2,3 and 4) are shown in the figure as well. Note that the q profile is multiplied by 10 in fig.2 to scale it to the plot. The q profile was calculated from the measured T_e and n_e profiles and neoclassical plasma conductivity assuming an uniform distribution of Z_{eff} in the plasma column. These minima correspond to rotating islands in plasma which are shown in more details in fig. 3.

Fig. 3 presents constant levels of T_e, n_e and p_e plotted along z direction and time restricted by two periods of DED current in the analysis interval from 2.5002 to 2.5024 s. The position of q values are marked in the right hand sides of the plots.

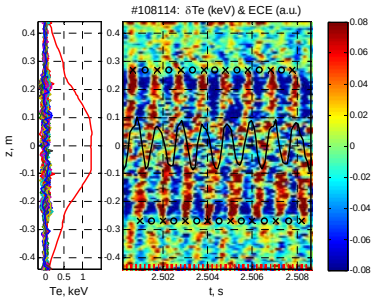

Fig. 1a
T_e oscillations in islands

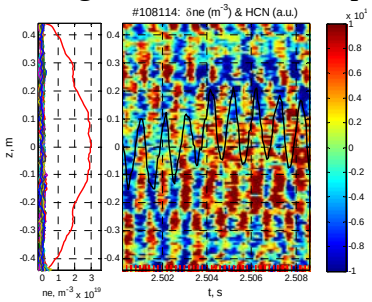

Fig. 1b
n_e oscillations in islands

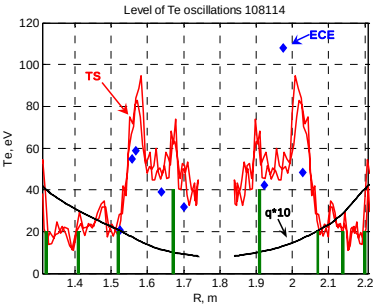

Fig 2
T_e, oscillations from TS and ECE

The levels are calculated using 43 T_e and n_e profiles measured during ~9 DED periods. All these measurements have been collected inside the analysis interval by shifts of measurements in multiple periods. Then the data were interpolated in time to get smooth variations of the plasma parameters and lower statistical errors (~1% for T_e and ~ 0.5% for n_e in the plasma core).

The green bold lines in fig.3 mark the borders of islands. Red and blue lines in the island interiors indicate higher and lower local parameters correspondingly. The interior lines of the islands are collected periodically inside a compact space called x-points where the magnetic lines are thought to reconnect. Colour lines in the central region inside the q=1 magnetic surface (|z|<0.1 m) are not necessarily represent the island structure at the line locations. These lines may have the same level as in the real islands located elsewhere nearby.

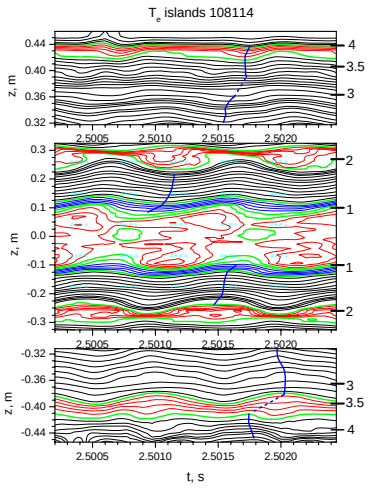

Fig.3a
Variations of T_e profiles

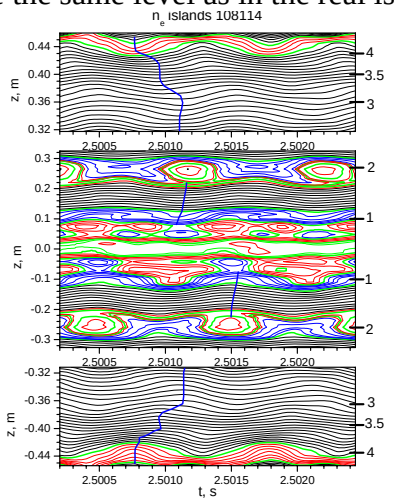

Fig.3b
Variations of n_e profiles

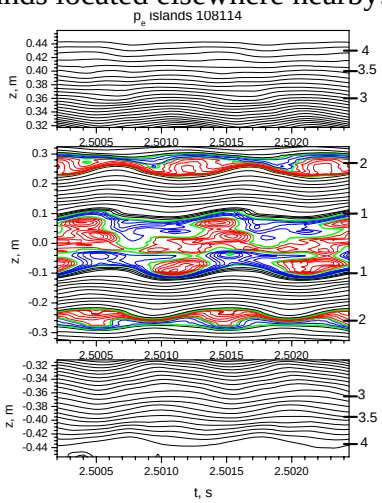

Fig.3c
Variations of p_e profiles

Island structure

The largest island is located in the magnetic surface with q=2 (m/n=2/1)and has the full width ~8 cm. The space-time structure of p_e (Fig.3c) most resembles the classical

symmetrical shape of the magnetic perturbations in islands [6]. The o-point of the p_e island overlaps with the o-points of T_e and n_e island structures.

Electron density has a local maximum in the o-point which is ~3% higher than the average density in the magnetic surface. The lines of constant density indicate an island structure with stretched x-point shifted to the plasma centre by 2 cm. This island structure alternates periodically. Its an embedded island having lower n_e in its o-point and stretched x-point shifted from the plasma centre by 2 cm. These two asymmetrical islands form a symmetrical structure which topology differs from the topology of the classical islands. The change of the island topology may relate to screening currents flowing in the tokamak vessel or neighbouring plasma regions [7].

The structure of T_e in the island region is somewhat between these later two structures. Embedded islands in the temperature structure are hardly seen (fig. 3a), but the x-point of the main T_e island is also stretched and shifted by 2 cm to the plasma edge. A similar shift of the T_e x-point to the plasma edge was measured in ASDEX UPGRADE by ECE diagnostic [8].

Thus, some quantity in the set of T_e, n_e and p_e appears to be not a functions of the magnetic flux around the x-point. Decoupling the local plasma parameters and the magnetic flux is commonly accounted for the competition of the parallel and perpendicular transport at the island separatrix [9]. But this theory does not predict so large decoupling region as well as stretching and splitting the T_e and n_e. x-points.

The structures of the island at the q=1 magnetic surface are masked by less certain relationship between the z-coordinate and the minor plasma radius, nevertheless they look generally similar to the structure of m/n=2/1 island.

An island at the plasma edge which rotates synchronically with the DED perturbations is visible in fig.3b. T_e perturbations at the edge are not detected because the TS system is less sensitive to lower T_e.

Smaller islands in plasma are masked by wavy variations of plasma parameters penetrating from larger islands. The small islands become apparent from the analysis of the phase shifts of the constant level curves. The blue vertical curves in fig.3b come through local maxima of n_e. The maxima are in phase with m/n=2/1 island at |z|~0.3 m, but when the curves approach the q=3 surface they change the direction and shift by ~0.15 ms having passed the q=3 region. Such a jump is repeated at the next rational surface q=4. These jumps can be accounted for island-like perturbations of n_e at the q=3 and q=4 magnetic surfaces. The time shifts give an estimation of the phase shift of these perturbations in respect to the island at q=2. The spatial shifts of the curves give an estimation of the full widths of the hidden islands which is ~1-1.5 cm.

Similar curves in T_e plot (fig. 3a) indicate an island at q=7/2, but hardly give any indication of T_e islands at q=3 and q=4 surfaces.

So, a significant difference between T_e and n_e structures has been found both for large and small rotating magnetic islands in the TEXTOR plasma.

Island rotation and phase delays

In the toroidal geometry, the phase delay of helical perturbations of magnetic field is given by [10]:

$$\Delta\Psi = n(\phi_2 - \phi_1)+m(\theta_2 - \theta_1)-m\,\delta(\sin\theta_2 - \sin\theta_1),\ \delta=r/R(\beta_p+l_i/2+1) \qquad (1)$$

Here (ϕ_1, θ_1) and (ϕ_2,θ_2) are the toroidal and poloidal angles of the measurement points located in the same magnetic surface. The toroidal correction δ is essential for the TEXTOR plasma and should be taken into account in the external part of the plasma column.

The TS diagnostic on TEXTOR allows the measurement of the phase delay between upper and lower points of a magnetic surface when island rotate through the TS measurement chord. In this way, TS diagnostic can provide high resolution profiles of the phase delay and rotation velocity of the island structure (T_e, n_e and p_e) along the plasma minor radius. The

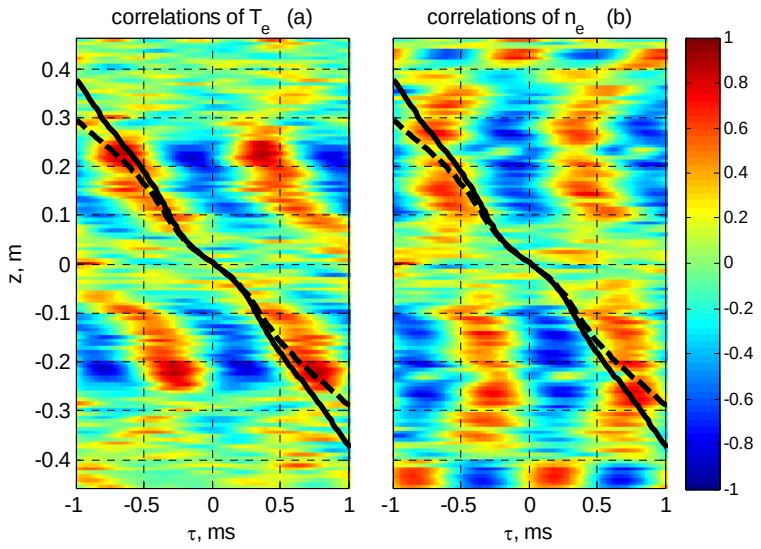

Fig. 4
Time-radial plots of Te and ne correlations

comparison of the experimental radial phase delay profiles with the calculated one (1) can point out plasma parameters which less coupled with the helical magnetic perturbations.

The delays of T_e, n_e and p_e are found with the use of the normalized correlation function in the time interval from -1 to 1 ms at a time step ~0.02 ms by interpolating the TS data. The correlations are shown in fig. 4 for the of T_e and n_e variations. The experimental phase delays of rotating T_e and n_e structures between upper and lower parts of the TS chord is traced along the red regions in the plots of fig. 4. Black dash and solid curves in the figure present the time delays of a magnetic perturbation rotating in the toroidal direction in the cylindrical and toroidal approximations correspondingly. The *n* number in the calculations was assumed to be 1 and the m number was equal to the local q value. The correctness of the assumption inside the q=2 magnetic surface is confirmed by a coincidence of the calculated delay and the measured delay of Te variations (fig 4.a). Behind the q=2 surface the assumption is not valid anymore because the rotation is driven buy *n=2* helical modes. This *n* number is estimated from the position of the region of high correlated Te oscillations (z=0.5 m, τ=- 0.5 ms).

The n_e rotating structures are less coupled with the helical magnetic perturbations as shown in fig. 4b. Therefore it is the density structure that is supposed to be not longer a function of the magnetic flux around the x-points of magnetic islands in TEXTOR.

Acknowledgments

This work was supported by NWO-RFBR Centre-of-Excellence grant 047.018.002. This work, supported by the European Communities under the Contract of Association between EURATOM-FOM, was carried out within the framework of the European Fusion Programme. The views and opinions expressed herein do not necessarily reflect those of the European Commission.

References

1 Special Issue, Fusion Eng. Design 37 (1997) 335, edited by K.H. Finken
2 M.Yu.Kantor, et al, Plasma Phys. Control. Fusion 51 (2009) 055002.
3 M.Yu.Kantor et al, Proc. of the 36th EPS. Sofia, Bulgaria, ECA Vol.33D, P-1.184 (2009)
4 H.J. van der Meiden et al. Rev. Sci. Instrum. 75 (2004) 3849
5 G.Waidmann, P.C. de Vries and A.Krämer-Flecken Rev. Sci. Instrum. 68 (1997) 492
6 R. Fitzpatrick, Nucl. Fusion 33, 1049 (1993)
7 M.Schittenhelm and H.Zohm, Nuclear Fusion, 37, 1255 (1997)
8 W.Suttrop et al. Nuclear fusion, 37, 120, (1997)
9 B.P. van Milligen et al., Nuclear Fusion 33, 1119 (1993)
10 M.Kikuchi. Nuclear fusion, 26, 101, (1986)